Collisional broadening and shifting parameters of the Raman Q branch of H_2 perturbed by N_2 determined from speed-dependent line profiles at high temperatures

P. M. Sinclair, J. Ph. Berger, X. Michaut, R. Saint-Loup, R. Chaux, and H. Berger
Laboratoire de Physique, Université de Bourgogne, 21000 Dijon, France

J. Bonamy and D. Robert
Laboratoire de Physique Moléculaire, Université de Franche-Comté, 25030 Besançon Cedex, France
(Received 14 December 1995)

The broadening and shifting of the Q branch of H_2 diluted in N_2 are studied at temperatures between 300 and 1200 K. (i) In order to account for the observed anomalies (asymmetric profiles and nonlinearity of the linewidth versus perturber concentration), the results are interpreted using a speed-dependent model in its general form. This model introduces the speed dependence of the shift and the broadening. In contrast with the previous H_2–rare-gas studies, the high-temperature measurements prove the necessity to include speed-dependent broadening that was ignored in the previous studies. (ii) Concomitantly, we report as well pure H_2 results including Raman frequencies for the $Q(7–9)$ lines and broadening and shifting results at 800 and 1200 K. A consistent set of data is deduced for H_2-N_2 up to 1200 K and the proposed model would be pertinent at higher temperatures for combustion applications. [S1050-2947(96)06907-7]

PACS number(s): 33.70.−w

I. INTRODUCTION

H_2 has recently been used as a probe molecule for spectroscopic combustion diagnostics [1]. In a typical H_2 coherent anti-Stokes Raman spectroscopy (CARS) experiment several lines are measured in the vibrational Q branch or pure rotational S branch. Since the lines are well separated the peak heights of individual lines can be measured. At low densities the lines are Doppler broadened; the ratios of peak heights are given by the Boltzmann distribution and the extraction of the temperature is straightforward. But above approximately one atmosphere, the lines are predominantly collision broadened. The area under a collision-broadened CARS line is inversely proportional to the linewidth Γ, and thus the peak height scales as Γ^{-2}. The situation is further complicated since the broadening depends on the perturber type. In a typical H_2-air flame, the major perturbers are N_2, H_2O, CO_2, and CO. We have measured the broadening of H_2 in the dominant perturber N_2 between 300 and 1200 K with the aim of extrapolating these results to flame temperatures of the order of 2000 K. We present first (Sec. II) a discussion of speed-dependent models that have been used to describe the spectra of H_2 perturbed by rare gases. We then give, in Sec. III, a brief description of the experimental apparatus followed by the experimental results and discussion (Sec. IV). The conclusions are given in Sec. V.

II. SPEED-DEPENDENT LINE PROFILES

The first precise measurements of H_2 perturbed by foreign gases were studies of H_2–rare-gas mixtures [2,3]. Two variations from the normal line-shape theories were observed. First, it was found that the line profile becomes asymmetric for low H_2 concentrations and that this asymmetry increases with temperature. Second, the total linewidth increases nonlinearly with the perturber concentration. These results were explained using speed-dependent line-shape models [2–6].

In the first experimental studies of speed-dependent line profiles both speed-dependent broadening and speed-dependent shifting were included in the models [7,8]. Recent results in CO [9] have been explained using models that include only speed-dependent broadening, whereas in the studies of H_2 it was assumed that only the speed dependence of the line shift was important. In this latter case the models predict an inhomogeneous broadening due to the *speed*-dependent shift analogous to the inhomogeneous broadening due to the *velocity* dependence [5] in the Doppler effect. But, since the Boltzmann distribution of *speeds* is not symmetric, the inhomogeneous profile is broadened asymmetrically. Further, analogous to the Dicke narrowing of Doppler profiles (due to *velocity*-changing collisions) the speed-dependent profile is narrowed by *speed*-changing collisions. For a light radiator in a bath of heavy perturbers the rate of speed-changing collisions decreases, and therefore the inhomogeneous broadening increases with the perturber concentration. When speed-dependent broadening is added to the model, the greatest effect is an increase in the asymmetry of the inhomogeneous profiles [10].

The general speed-dependent model of Robert *et al.* [4] includes three types of collisions: dephasing collisions (D), speed-changing collisions (SC), and collisions that are both speed changing and dephasing (SCD). The line profile is given in an analytic form

$$I(\omega)=\pi^{-1}\mathrm{Re}\left\{\frac{\langle[i\omega+F(v)]^{-1}\rangle}{1-\nu_{\mathrm{SC}}\langle[i\omega+F(v)]^{-1}\rangle-\langle[\nu_{\mathrm{SCD}}-\gamma_{\mathrm{SCD}}(v)-i\delta_{\mathrm{SCD}}(v)][i\omega+F(v)]^{-1}\rangle}\right\}, \quad (1)$$

where $F(v)=\nu_{SC}+\nu_{SCD}+\gamma_D(v)+i\,\delta(v)$, ω is the detuning frequency, and ν denotes a collision frequency. In Eq. (1), $\langle\ \rangle$ means an average over the radiator speed. In Ref. [3] two limiting cases of the model were used. If there are no SCD collisions then the model of Farrow *et al.* [2] is obtained (FRSR model). The other limit assumes no SC collisions and was called the Robert-Thuet-Bonamy-Temkin (RTBT) model. We have investigated both models and find, as in Ref. [3], that they describe the data equally well. Thus in our analysis we are unable to distinguish between SCD and SC collisions. For brevity we have chosen to present our analysis using only the RTBT model. The reader is referred to Refs. [2, 3] for more details of the FRSR model.

For the RTBT model the fraction $x(T)$ of SCD collisions is defined by

$$x(T)=\nu_{SCD}/\nu_{tot},\quad \nu_{tot}=\nu_{SCD}+\nu_D, \tag{2}$$

where ν_{tot} is the total collision frequency. The collisional broadening and shifting are given by

$$\gamma_{coll}(v)=\gamma_D(v)+\gamma_{SCD}(v),\quad \delta_{coll}(v)=\delta_D(v)+\delta_{SCD}(v). \tag{3}$$

It has been shown that $\delta_{coll}(v)$ can be obtained directly from measurements of the temperature dependence of the shift coefficient, which was found [3] to obey the law

$$\delta_{coll}(T)=\tilde{\delta}\sqrt{T}+\delta_0. \tag{4}$$

Similarly the collisional broadening varies linearly with temperature:

$$\gamma_{coll}(T)=\tilde{\gamma}T+\gamma_0. \tag{5}$$

The relationships between the speed-dependent quantities defined in Eq. 3 and the temperature coefficients defined in Eqs. 4 and 5 have been derived in Ref. [3] and are repeated below:

$$\gamma_{coll}(y,T)=\frac{3\tilde{\gamma}\pi\mu\overline{v_p^2}}{8k}\,e^{-y^2}M(\tfrac{5}{2},\tfrac{3}{2},y^2)+\gamma_0, \tag{6}$$

$$\delta_{coll}(y,T)=\tilde{\delta}\sqrt{T}\sqrt{\mu/m_p}e^{-y^2}M(2,\tfrac{3}{2},y^2)+\delta_0, \tag{7}$$

where y is the reduced speed ($y=v/\tilde{v}_p$), $\tilde{v}_p$ is the most probable perturber speed ($\tilde{v}_p=\sqrt{2kT/m_p}$), $\overline{v_p}$ is the average perturber speed ($\overline{v_p}=\sqrt{8kT/\pi m_p}$), μ is the reduced mass, m_p is the perturber mass, and $M(\,)$ is the confluent hypergeometric function. In the following analysis we allow x to vary linearly with temperature:

$$x(T)=\tilde{x}\,T+x_0. \tag{8}$$

The temperature dependence of x is not based on physical considerations but is an empirical form based on the fact that in Ref. [3] x was found to be constant or vary only slightly with temperature.

For the general RTBT model seven parameters $[\tilde{x},x_0,\tilde{\delta},\delta_0,\tilde{\gamma},\gamma_0,\nu_{tot}]$ are needed. But the temperature shift coefficients $\tilde{\delta}$ and δ_0 can be obtained directly from the data, independently of the model, leaving five unknown parameters. The total collision frequency is set equal to the velocity changing frequency β, defined by Rautian and Sobel'man [5] as

$$\beta=kT/mD, \tag{9}$$

reducing the number of parameters to four. Of course, for a mixture, the parameters $\delta_{coll}(v)$, $\gamma_{coll}(v)$, and x are the concentration weighted sums of the pure H_2 and H_2-N_2 values. But we assume, as was done in Ref. [3], that the broadening of pure H_2 is completely homogeneous, due to the large speed changing rate, and thus $x_{H_2}=1$; the collisional broadening is equal to the total broadening and can be determined directly from the experiments. In the following sections the pure H_2 broadening and shifting parameters are calculated from data presented in Ref. [3] and results reported here. The speed-dependent model is then used to fit the data to determine the H_2-N_2 parameters $[\tilde{x},x_0,\tilde{\gamma},\gamma_0]$.

We have found that the speed-dependent broadening, which has been ignored in the H_2–rare-gas studies, must be included to describe the H_2-N_2 results. The importance of this term will be shown by comparing models with [RTBT-$\gamma(v)$] and without (RTBT) the speed-dependent broadening term.

III. EXPERIMENT

The inverse Raman spectrometer used in these experiments has been described in Ref. [3]. A brief description of the system and some modifications are given below.

The pump laser is a pulse amplified cw ring dye laser operating at 655 nm. The pulse duration was 4 ns, giving an instrumental width of 8×10^{-3} cm^{-1} full width at half maximum (FWHM). The average power at a 25 Hz repetition rate was usually between 5 and 10 mW (peak powers between 50 and 100 kW). The probe laser is a frequency-stabilized argon-ion laser, operating at 514 nm, and providing approximately 200 mW at the gain cell.

The sample cell was the same design as used previously, except that it was constructed from inconel™, which is more temperature resistant than stainless steel, allowing the new cell to reach temperatures of 1200 K.

Measurements were made at temperatures of 296, 800, and 1200 K and at densities between 8 and 10 amagat, except for a few which were made at 5 amagat. At 800 and 1200 K the pump and probe beams were crossed at a small angle in the 30-cm-long sample cell so that the Raman signal comes only from a region near the center of the cell where the temperature is constant. Temperature and pressure measurements have been previously described in detail [3].

The virial coefficient for H_2 mixtures is given by

$$B_T=c_{H_2}^2B_{H_2\text{-}H_2}+2c_{H_2}c_{N_2}B_{H_2\text{-}N_2}+c_{N_2}^2B_{N_2\text{-}N_2}. \tag{10}$$

The coefficients B were derived from experiments [11] when possible, or otherwise calculated according to Ref. [12]. The largest virial correction to the density was 1.5%.

IV. RESULTS

Most of the experiments were done at densities between 8 and 10 amagat, well above the Dicke minimum [13] of 1 to

TABLE I. Transition frequencies (cm^{-1}) for the $Q(J)$ lines at zero density. The experimental values have been corrected by adding the estimated Stark shifts which are given in the first set of parentheses. The statistical uncertainties are given in the second set of parentheses.

J	Experiment	Interpolation	Previous[a]	(Expt.)-(Prev.)	Theory[b]	(Expt.)-(Theory)
6		4039.492	4039.52		4039.481	
7	4000.055(+1)(1)		3999.87	0.19	4000.046	0.009
8	3955.640(+2)(1)		3956.04	−0.38	3955.633	0.007
9	3906.479(+2)(1)		3906.31	0.17	3906.474	0.005

[a]Reference [15].
[b]Reference [16].

3 amagat. In this regime there remains a residual Doppler component and the linewidth without the Doppler broadening is given (in cm^{-1}) by

$$\Gamma(T)=\Gamma^{\mathrm{obs}}(T)-\frac{2\pi D(T)\nu_R^2}{c\rho}, \tag{11}$$

where $\Gamma^{\mathrm{obs}}(T)$ is the half width at half maximum of the observed spectrum, $D(T)$ is the diffusion constant, c the speed of light, and ν_R the Raman frequency. In this expression $\Gamma^{\mathrm{obs}}(T)$, $\Gamma(T)$, and ν_R are expressed in cm^{-1}, and $D(T)$ in cm^{-2} amagat s^{-1}. The broadening coefficients γ are defined as $\gamma=\Gamma/\rho$, where ρ is the density in amagat units.

The correction for the Doppler component is almost negligible at 10 amagat but can be up to 7% at 5 amagat. It should be mentioned that Eq. (11) is strictly valid only for a homogeneously (collisionally) broadened profile. For an inhomogeneous profile each speed class will have a modified Doppler profile and Eq. (11) is no longer valid. But since the Doppler correction is small, the error made in using this formula is not significant.

A. Pure H_2

With the new inconel™ gas cell we have been able to increase the temperature to 1200 K, 200° higher than the previous cell. At 1200 K we have measured ten [$Q(0–9)$] lines in pure H_2, four more than in previous experiments.

We have measured the line frequencies at a density of approximately 10 amagat using an absolute frequency wavemeter. For the $Q(0–5)$ lines the shift was calculated relative to the zero density Raman frequencies reported by Rahn and Rosasco [14], but for the $Q(6–9)$ lines there are no precise values in the literature. For the $Q(7–9)$ lines we have measured the line frequencies at several densities between 1 and 8 amagat. The data have been fitted to straight lines in order to determine the zero density Raman frequencies, which are reported in Table I. Unfortunately, due to the failure of a cell window, the $Q(6)$ line was not measured.

The pump laser peak power was typically between 50 and 100 kW for the $Q(0–5)$ lines and up to 200 kW for the $Q(6–9)$ lines. For a power of 100 kW, under similar focusing conditions, Rahn and Rosasco [14] have measured a Stark shift of approximately 1.4×10^{-3} cm^{-1}. The $Q(7–9)$ Raman transition frequencies reported in Table I have been corrected for the Stark shift, using a coefficient of 1.4×10^{-5} cm^{-1} kW. The $Q(6)$ transition frequency was determined from a third-order polynomial fit to the $Q(0–5)$ values taken from Ref. [14] and our $Q(7–9)$ values. We have also shown in Table I the experimental values of Dabrowski [15] obtained using spontaneous Raman scattering and the theoretical values of Wolniewicz [16]. Our values are an order of magnitude more precise than the previous experimental values and are in good agreement with the theory.

For the calculation of the shift coefficients we have not corrected any of our line frequency measurements for the Stark shift. For the $Q(0–5)$ lines our shift coefficients were calculated relative to the Stark corrected zero density values of Rahn and Rosasco [14]. We estimate that this introduces an error of only 10^{-4} cm^{-1} amagat. For some of the higher J lines, $Q(6–9)$, a higher pump power was used but in this case all shift measurements were made relative to the Raman frequencies measured in our laboratory, which have not been corrected for the Stark shift. Since all measurements for a single line were made with similar pump powers, the Stark-shift errors cancel when calculating the density shift coefficient. In Table II we report the pure H_2 shifting and broadening coefficients at 800 and 1200 K.

B. Line shifting in H_2-N_2 mixtures

In Fig. 1 we show a $Q(3)$ line profile of a 10% H_2 mixture at 1200 K. The asymmetry of the profile is highlighted by comparison to the symmetric Lorentzian fit also shown in the figure. In the study of H_2 perturbed by rare gases it was found that, due to the asymmetry, the line position must be

TABLE II. Experimental collisional shifting and broadening coefficients (expressed in 10^{-3} cm^{-1} $amagat^{-1}$) for pure H_2. The numbers in parentheses indicate the estimated experimental uncertainties.

	Shifting		Broadening	
J	800 K	1200 K	800 K	1200 K
0		10.3(2)		9.3(2)
1		11.0(2)		5.37(8)
2		11.7(2)		6.1(1)
3		11.5(2)		6.0(1)
4		12.3(2)		5.3(1)
5		12.5(2)		5.0(1)
6	7.8(2)	13.2(2)	2.9(1)	4.4(1)
7	8.2(2)	13.6(2)	2.5(1)	4.0(1)
8		13.7(2)		3.5(1)
9		14.0(2)		3.5(1)

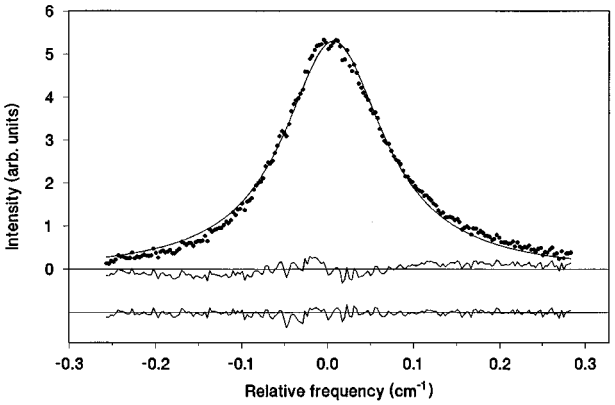

FIG. 1. Profile of the $Q(3)$ line of a mixture of 10% H_2 in N_2 at 1200 K. The dots are the experimental data points, the solid line is the best-fit symmetric Lorentzian, and the residual (expt.-fit) is shown below. The data have also been fit to the RTBT-$\gamma(v)$ model (fit not shown) and the residual has been offset for clarity. The residual to the Lorentzian shows asymmetric structure above the level of the noise while the residual to the RTBT-$\gamma(v)$ model is structureless.

determined from the center of gravity of the profile [3]. In Fig. 2 we show the shifting of the $Q(1)$ line as a function of N_2 concentration, at all temperatures studied. For comparison we have shown results from both center-of-gravity and Lorentzian fits. At 296 K the profiles are symmetric except at the smallest concentrations studied. As the temperature is increased the profiles become more asymmetric and at 1200 K the Lorentzian model results in an error even for relatively high (50%) H_2 concentrations.

For the strong $Q(1)$ and $Q(3)$ lines, the shift, determined from the center of gravity, varies linearly with concentration

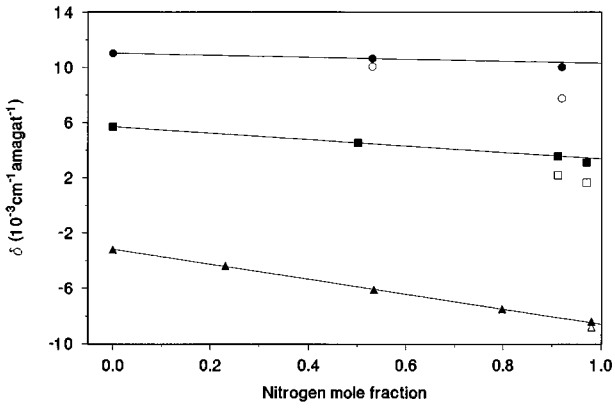

FIG. 2. Shifting coefficient for the $Q(1)$ line has been plotted against the perturber concentration. The filled symbols are the values obtained from the center of gravity of the profiles while the open symbols are the results obtained from Lorentzian fits. Data are shown for three temperatures: triangles, 296 K; squares, 800 K; and circles, 1200 K. The Lorentzian results are shown only to demonstrate the significant errors that can be obtained from this model. The center-of-gravity data have been fit to straight lines using only the results for mixtures with greater than 20% H_2 since the high dilution results are very sensitive to errors due to instrumental asymmetries. The extrapolated infinite dilution shift coefficients are reported in Table III.

TABLE III. Experimental collisional line shifting coefficients δ_{coll} (expressed in 10^{-3} cm^{-1} amagat^{-1}) for H_2 infinitely diluted in N_2. The numbers in parentheses indicate the estimated experimental uncertainty.

J	296 K	800 K	1200 K
0	−9.44(15)	−0.7(2)	4.6(3)
1	−8.59(10)	3.4(2)	10.3(3)
2	−8.05(15)	4.0(2)	12.3(4)
3	−7.84(15)	4.6(2)	12.1(3)
4	−7.67(25)	5.7(3)	14.1(5)
5		6.2(6)	14.5(5)
6		6.4(4)	14.3(5)
7		7.0(4)	14.8(6)
8			14.7(6)
9			15.2(8)

for all temperatures. But for the other less intense lines small instrumental effects become significant for the experiments done at low H_2 concentrations. To avoid systematic errors due to instrumental asymmetries we have not used the values obtained with less than 20% H_2 when fitting the data to extrapolate to 0% H_2. The extrapolated infinite dilution shift coefficients are shown in Table III. For the very weak $Q(8–9)$ lines at 1200 K the signal quality even for 50% mixtures was too low to find precisely the center of gravity. As a result there are possibly small systematic errors, estimated to be less than 0.5×10^{-3} cm^{-1} amagat, for the reported $Q(8–9)$ shift coefficients.

The shift coefficients for the $Q(0–4)$ lines have been plotted versus the square root of the temperature in Fig. 3. The accuracy of this simple law for H_2-N_2 is similar to that of the H_2–rare-gas case. So, the data have been fitted to straight lines and the coefficients are given in Table IV. These coefficients are used in the speed-dependent models described below. From Fig. 3 it can be seen that the extrapolated fits tend to converge to a single value of -13×10^{-3} cm^{-1} amagat at a temperature of approximately 170 K. Since all Q branch lines have the same shift at this temperature, we have used this value to estimate the shift coefficients for the $Q(5–7)$ lines.

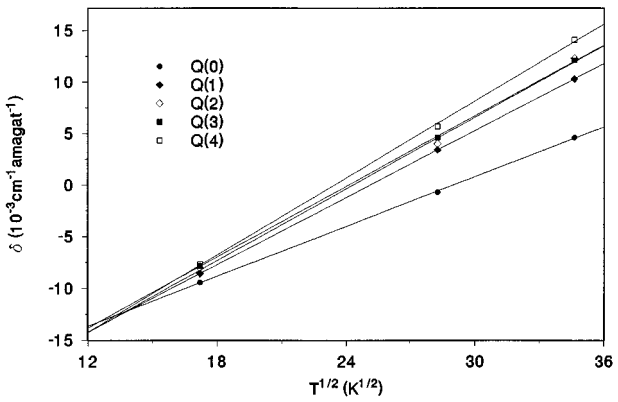

FIG. 3. Shifting of the $Q(0–4)$ lines is shown versus the square root of the temperature. The data have been fit to straight lines and the coefficients are reported in Table IV.

TABLE IV. Parameters δ and δ_0 of the expression $\delta_{\text{coll}}(T)=\tilde{\delta}\sqrt{T}+\delta_0$, fitted through a weighted least-squares procedure to the experimental H_2-N_2 line shifts. $\tilde{\delta}$ and δ_0 are in units of 10^{-3} cm^{-1} $amagat^{-1}$ $K^{-1/2}$ and 10^{-3} cm^{-1} $amagat^{-1}$, respectively.

	$Q(0)$	$Q(1)$	$Q(2)$	$Q(3)$	$Q(4)$	$Q(5)$	$Q(6)$	$Q(7)$
$\tilde{\delta}$	0.80(2)	1.08(1)	1.12(2)	1.14(2)	1.23(3)	1.27[a]	1.27[a]	1.30[a]
δ_0	−23.2(4)	−27.2(3)	−27.4(4)	−27.4(4)	−28.9(6)	−29.8[a]	−29.9[a]	−29.9[a]

[a]Estimated values, see text.

C. Line broadening in H_2-N_2 mixtures

As discussed in the Introduction, the speed-dependent models predict both nonlinear broadening and asymmetric profiles. The values of x and γ_{coll} can be found either by fitting the model to the experimental broadening coefficient γ versus perturber concentration or by fitting single profiles. To demonstrate the importance of speed-dependent broadening we discuss the analysis of the data by using the two methods of fitting and using both the RTBT and RTBT-$\gamma(v)$ models.

As the first step, let us consider only the first method of fitting applied to the $Q(J)$ lines. In Fig. 4 the experimental broadening coefficient γ [cf. Eq. (11)] is plotted versus N_2 concentration for the $Q(0)$ and $Q(1)$ lines. For the $Q(1)$ line it is clear that at all temperatures studied the broadening varies nonlinearly with N_2 concentration. This dependence is seen for all $Q(J)$ lines, except $Q(0)$, which is discussed separately below.

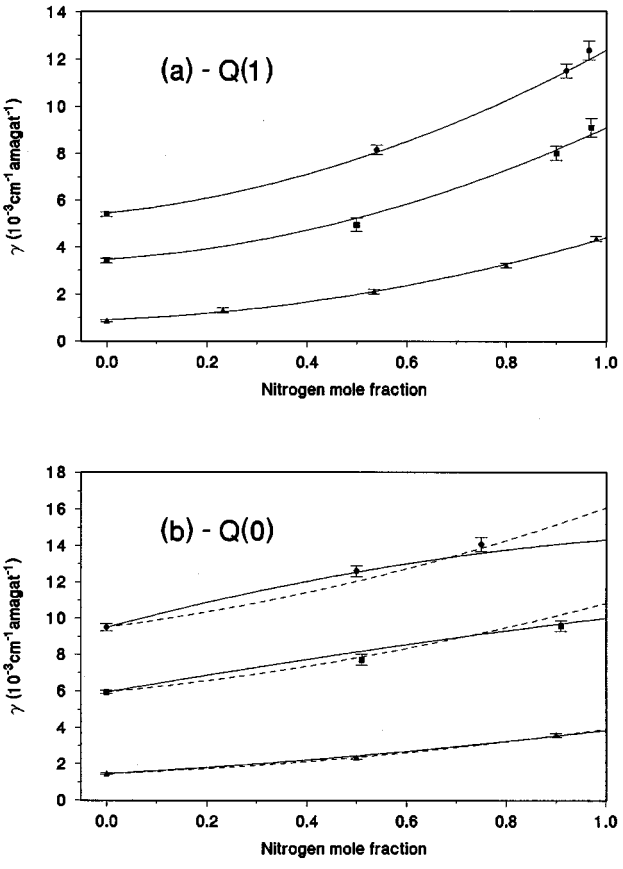

FIG. 4. Experimental broadening coefficients for the $Q(0)$ and $Q(1)$ lines are shown versus the perturber concentration. Data are shown for three temperatures: triangles, 296 K; squares, 800 K; and circles, 1200 K. (a) $Q(1)$: the RTBT-$\gamma(v)$ and RTBT model fits are indistinguishable and are shown by the solid lines. (b) $Q(0)$: the solid and dashed lines show the fits to the RTBT-$\gamma(v)$ and RTBT models, respectively.

The RTBT model requires the parameters δ_{coll} and β. The pure H_2 temperature shift coefficients for the $Q(0$–$5)$ lines were obtained from Ref. [3]. For the $Q(6)$ and $Q(7)$ lines they were estimated using the method discussed above for the $Q(5$–$7)$ H_2-N_2 results. The H_2-N_2 temperature shift coefficients are reported in Table IV. The velocity changing rates β were obtained using mass diffusion constants calculated following Ref. [12]. In Ref. [3] the velocity-changing rate for pure H_2 was calculated using the ''optical'' diffusion constant measured by Rahn *et al.* [17]. The choice of diffusion constant does have a small effect on the results of the RTBT model. In this work we have chosen to use the mass diffusion values for two reasons: (i) The physical meaning of the ''optical'' diffusion coefficients obtained from experiments is not well understood. Recent publications show that more theoretical work is probably needed to correctly interpret the experimental results (e.g., see Refs. [18, 19]). (ii) For consistency we would like to use the same basis for pure H_2 and for H_2-N_2. Since optical diffusion constants do not exist for the mixtures, this limits us to the mass diffusion values.

To demonstrate the importance of speed-dependent broadening, we discuss the analysis of the $Q(1)$ line in detail. The experimental broadening coefficients γ, as a function of concentration, at all three temperatures, were fitted simultaneously for the four parameters $[\tilde{x},x_0,\tilde{\gamma},\gamma_0]$ using both the RTBT and RTBT-$\gamma(v)$ models. The results are shown in Fig. 4(a); on the scale of the figure the two models are indistinguishable [note that this is true for all lines except $Q(0)$, which is shown in Fig. 4(b) and discussed in more detail below]. While the two models fit the data equally well, the ratio of collision frequencies x differs. The ratio was found to be temperature independent and to have values of 0.20 and 0.14 for the RTBT and RTBT-$\gamma(v)$ models, respectively. When speed-dependent collisional broadening is added to the model, it has the effect of narrowing the inhomogeneously broadened profiles. In order to compensate, a larger inhomogeneous broadening is needed and thus the speed-changing ratio x is reduced. While the significant change in the coefficient x is reason enough to warrant the inclusion of speed-dependent broadening, a much more important difference is found when individual profiles are analyzed, as shown below.

In a second step we have fitted individual profiles using the RTBT and RTBT-$\gamma(v)$ models. Since the accuracy of the line profile asymmetry is very important when determining the parameters using the second fitting method, false (instrumental) asymmetries would result in large errors. But we believe that the experimental results for the $Q(1)$ line are free

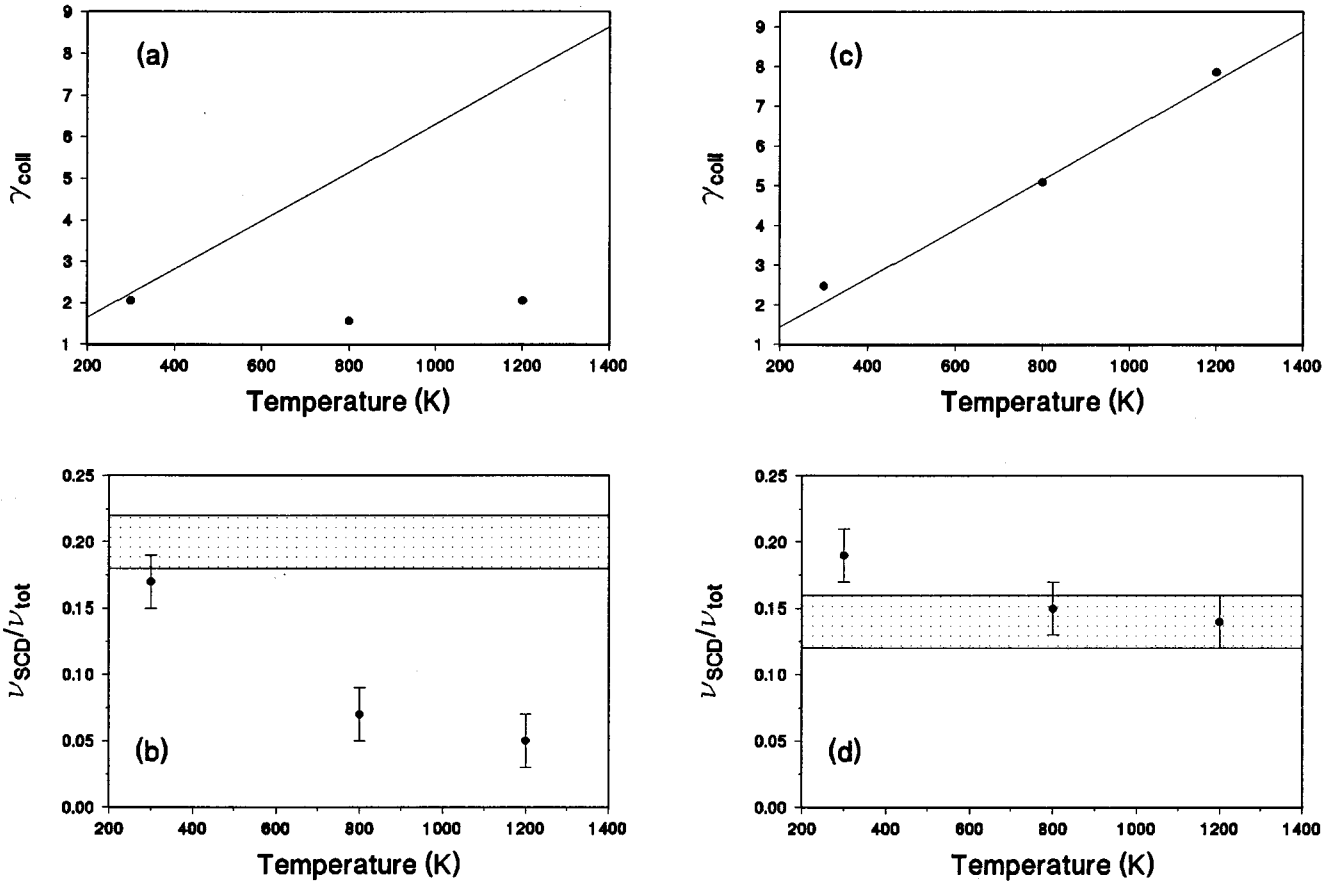

FIG. 5. All results are for the $Q(1)$ line. The straight lines (γ_{coll}) and shaded areas (ν_{SCD}/ν_{tot}) show the values obtained from fitting the experimental broadening versus concentration. The dots were obtained from single profile fits. (a) RTBT model results for γ_{coll}. (b) RTBT model results for ν_{SCD}/ν_{tot}. (c) RTBT-$\gamma(v)$ model results for γ_{coll}. (d) RTBT-$\gamma(v)$ model results for ν_{SCD}/ν_{tot}.

from instrumental asymmetries since the shift obtained from the center-of-gravity model is linear with perturber concentration (Fig. 2). We have fitted several spectra for 2–10 % H_2 in N_2 at all three temperatures. The results for x and γ_{coll} as well as values from the first fitting method are shown in Fig. 5. In Figs. 5(a) and 5(b) we show the results from the two fitting methods for the RTBT model. At room temperature the two methods are in agreement, but there are large disagreements at the higher temperatures. The first fitting method predicts a γ_{coll}, which increases with temperature while the second method gives a constant γ_{coll}. In Figs. 5(c) and 5(d) we show results from a similar analysis but using the RTBT-$\gamma(v)$ model. The two methods are in much better agreement now, although there is a slight discrepancy for the value of x obtained at room temperature.

Following the above analysis we have used the RTBT-$\gamma(v)$ model to fit the $Q(0,2–7)$ lines. For the $Q(2–4)$ lines we have fitted the four parameters $\tilde{x}, x_0, \tilde{\gamma}, \gamma_0$ and found that the temperature-dependent coefficient $\tilde{x}$ was negligible. For the other lines [$Q(0,5–7)$], x was fixed at the average value of 0.12 calculated from the $Q(1–4)$ lines. The coefficients are reported in Table V.

In a third step we have focused our attention on the $Q(0)$ line, which is of special interest, as can be seen from Fig. 4(b). We show the experimental broadening coefficient γ as well as the corresponding results from the RTBT and RTBT-$\gamma(v)$ models versus perturber concentration. While the two models fit the data equally well, the results are different: the RTBT-$\gamma(v)$ model predicts a change of the curvature as the temperature increases. To aid the interpretation of these results we show the results of several model calculations in Fig. 6. All the results in this figure were obtained using the set of parameters determined from the RTBT-$\gamma(v)$ model fit of the $Q(0)$ data at 1200 K [the data and fit are shown in Fig. 4(b)]. In Fig. 6 we show a solid line representing the experi-

TABLE V. Parameters $\tilde{\gamma}$ and γ_0 of the expression $\gamma_{coll}(T) = \tilde{\gamma} T + \gamma_0$ and ν_{SCD}/ν_{tot} found by fitting the total broadening versus perturber concentration using the RTBT-$\gamma(v)$ model.

J	ν_{SCD}/ν_{tot}	$\tilde{\gamma}$ (10^{-6} cm^{-1} amagat^{-1} K^{-1})	γ_0 (10^{-3} cm^{-1} amagat^{-1})
0	0.12[a]	13.9(6)	−1.1(2)
1	0.14(1)	6.2(2)	0.2(1)
2	0.09(1)	8.6(3)	−0.3(2)
3	0.13(2)	7.9(4)	−0.1(2)
4	0.13(1)	6.6(3)	−0.4(2)
5	0.12[a]	6.5(4)	−0.6(3)
6	0.12[a]	8(2)	−1(2)
7	0.12[a]	9(3)	−3(2)

[a]Fixed at average value obtained from $Q(1–4)$.

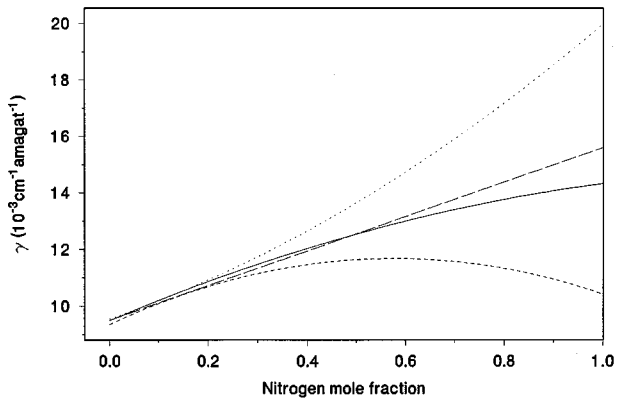

FIG. 6. RTBT-$\gamma(v)$ model results taken from Fig. 4(b) for the $Q(0)$ line at 1200 K have been replotted (solid line) along with the collisional broadening coefficient γ_{coll} determined from the same fit (long dashes). Also shown are predictions for γ obtained using the RTBT model (dots) and the RTBT-$\gamma(v)$ model, but with the speed-dependent shift suppressed (short dashes).

mental broadening γ versus perturber concentration and a straight dashed line representing the collisional broadening γ_{coll}. The surprising result is that at high dilution ratios the RTBT-$\gamma(v)$ model predicts broadening coefficients smaller than the collisional broadening. To further elucidate the problem we have done two simulations using the same model parameters. In one simulation we have suppressed the speed dependence of the collisional broadening (i.e., we have used the RTBT model) and in the other we have suppressed the speed dependence of shift. The results are shown in Fig. 6 and it is apparent that the speed-dependent shifting and broadening cause nonlinearities of opposite signs; the near linear dependence of the width, observed for the $Q(0)$ line at 800 and 1200 K, is due to the cancellation of the speed-dependent shifting and broadening effects. It should be noted that the effects do not completely cancel since the spectra are still highly asymmetric. In comparison to the other lines, the $Q(0)$ line is anomalous due to a smaller temperature shift and a larger temperature broadening coefficient, which results in relatively large speed-dependent broadening effects for this line. As a small aside, we note in Fig. 6 that when the speed-dependent shift is suppressed the calculation predicts that the broadening γ actually decreases slightly at high N_2 concentrations. This prediction could perhaps be tested by studying the pure rotational S branch of H_2 in mixtures since the pure gas spectra have shift coefficients one order of magnitude smaller than the Q branch [20] (at least at room temperature).

In the studies of H_2 perturbed by rare gases no significant limitations of the speed-dependent models were found. In Ref. [3] the values of x and γ_{coll} were found from the variation of the broadening γ with the perturber concentration. We have fitted some of the single H_2-Ar profiles used in Ref. [3] and we find small discrepancies similar to those found in the present work. In Ref. [2] the asymmetries were well reproduced by the FRSR model, while in the present work we find that speed-dependent broadening must be included in both the RTBT and FRSR models. We believe that the discrepancy lies in the difference between the model used for the speed-dependent shift cross section used both here and in Ref. [3] and that used in Ref. [2]. This has been discussed previously in Ref. [3].

V. CONCLUSIONS

We have measured the broadening and shifting of H_2 perturbed by N_2 at temperatures between 300 and 1200 K. Using the center of gravity of the line profiles as a measure of the line position we find that the shift coefficient varies linearly with perturber concentration. Further, we find that the shift coefficient for H_2 infinitely diluted in N_2 varies linearly with the square root of the temperature.

We have observed that the experimental width varies nonlinearly with perturber concentration and that the profiles become asymmetric for high perturber concentrations. The data have been described using the speed-dependent model of Robert *et al.* [4] and we show that the speed-dependent broadening term cannot be neglected. There are two reasons for including speed-dependent broadening in the model. First, the inclusion of this term significantly changes the model predictions for highly diluted mixtures. Second, we have shown that consistent results can be obtained only if this term is included. Specifically, this term is needed in order to fit both the experimental width versus concentration and single profiles with a single set of parameters.

The aim of this research is to obtain broadening coefficients that can be used in the analysis of spectroscopic combustion data. To obtain accurate broadening values, we must consider all the relevant perturbers and then use the speed-dependent model to predict the experimental width at the combustion temperature. Preliminary results using H_2-N_2 and H_2-H_2O [21] data have shown good agreement with H_2-air flame results [1]. Further work is needed to improve the precision of the H_2-H_2O results and possibly measure H_2-CO and H_2-CO_2 mixtures.

ACKNOWLEDGMENTS

The authors are grateful to V. Bergmann and W. Stricker for stimulating discussions about CARS spectroscopy of flames. P. M. Sinclair would like to thank the Conseil Regional de Bourgogne for financial support during this research. The Laboratoire de Physique de l'Université de Bourgogne is a Unité de Recherche Associée au CNRS No. 1796 and the Laboratoire de Physique Moléculaire is a Unité de Recherche Associée au CNRS No. 772.

[1] W. Stricker, M. Woyde, R. Lückerath, and V. Bergmann, Ber. Bunsenges. Phys. Chem. **97**, 1608 (1993).

[2] R. L. Farrow, L. A. Rahn, G. O. Sitz, and G. J. Rosasco, Phys. Rev. Lett. **63**, 746 (1989).

[3] J. Ph. Berger, R. Saint-Loup, H. Berger, J. Bonamy, and D. Robert, Phys. Rev. A **49**, 3396 (1994).

[4] D. Robert, J. M. Thuet, J. Bonamy, and S. Temkin, Phys. Rev. A **47**, 771 (1993).

[5] S. G. Rautian and I. I. Sobel'man, Usp. Fiz. Nauk **90**, 209 (1967) [Sov. Phys. Usp. **9**, 701 (1967)].
[6] J. W. Forsman, J. Bonamy, D. Robert, J. Ph. Berger, R. Saint-Loup, and H. Berger, Phys. Rev. A **52**, 2652 (1995).
[7] M. Harris, E. L. Lewis, D. McHugh, and I. Shannon, J. Phys. B **17**, L661 (1984).
[8] I. Shannon, M. Harris, D. R. McHugh, and E. L. Lewis, J. Phys. B **19**, 1409 (1986).
[9] P. Duggan, P. M. Sinclair, A. D. May, and J. R. Drummond, Phys. Rev. A **51**, 218 (1995).
[10] P. R. Berman, J. Quant. Spectrosc. Radiat. Transfer. **12**, 1343 (1972).
[11] J. H. Dymond and E. B. Smith, *The Virial Coefficients of Pure Gases and Mixtures* (Clarendon, Oxford, 1980).
[12] J. O. Hirschfelder, C. F. Curtiss, and R. B. Bird, *Molecular Theory of Gases and Liquids* (Wiley, New York, 1964).
[13] R. H. Dicke, Phys. Rev. **89**, 472 (1953).
[14] L. A. Rahn and G. J. Rosasco, Phys. Rev. A **41**, 3698 (1990).
[15] I. Dabrowski, Can. J. Phys. **62**, 1639 (1984).
[16] L. Wolniewicz, J. Chem. Phys. **99**, 1851 (1993).
[17] L. A. Rahn, R. L. Farrow, and G. J. Rosasco, Phys. Rev. A **43** 6075 (1991).
[18] L. Demeio, S. Green, and L. Monchick, J. Chem. Phys. **102**, 9160 (1995).
[19] P. Duggan, P. M. Sinclair, M. P. Le Flohic, J. W. Forsman, R. Berman, A. D. May, and J. R. Drummond, Phys. Rev. A **48**, 2077 (1993).
[20] M. P. Le Flohic, P. Duggan, P. M. Sinclair, J. R. Drummond, and A. D. May, Can. J. Phys. **72**, 186 (1994).
[21] J. Ph. Berger, thèse de doctorat, Université de Bourgogne, Dijon, France, 1994 (unpublished).